Interactive effects of shifting body size and feeding adaptation drive interaction strengths of protist predators under warming

Temperature adaptation of feeding

K.E.Fussmann [1,2], B. Rosenbaum [2, 3], U.Brose [2, 3], B.C.Rall [2, 3]

[1] J.F. Blumenbach Institute of Zoology and Anthropology, University of Göttingen, Berliner Str. 28, 37073 Göttingen, Germany

[2] German Centre for Integrative Biodiversity Research (iDiv), Halle-Jena-Leipzig, Deutscher Platz 5e, 04103 Leipzig, Germany

[3] Institute of Ecology, Friedrich Schiller University Jena, Dornburger-Str. 159, 07743 Jena, Germany

Corresponding author: Katarina E. Fussmann

telephone: +49 341 9733195

email: katarina.fussmann@biologie.uni-goettingen.de

Keywords: climate change, functional response, body size, temperature adaptation, activation energies, microcosm experiments, predator-prey, interaction strength, Bayesian statistics

Paper type: Primary Research

Abstract

Global change is heating up ecosystems fuelling biodiversity loss and species extinctions. High-trophic-level predators are especially prone to extinction due to an energetic mismatch between increasing feeding rates and metabolism with warming. Different adaptation mechanisms such as decreasing body size to reduce energy requirements (morphological response) as well as direct effects of adaptation to feeding parameters (physiological response) have been proposed to overcome this problem. Here, we use protist-bacteria microcosm experiments to show how those adaptations may have the potential to buffer the impact of warming on predator-prey interactions. After adapting the ciliate predator *Tetrahymena pyriformis* to three different temperatures (15°C, 20°C and 25°C) for approximately 20 generations we conducted functional response experiments on bacterial prey along an experimental temperature gradient (15°C, 20°C and 25°C). We found an increase of maximum feeding rates and half-saturation densities with rising experimental temperatures. Adaptation temperature had on average slightly negative effects on maximum feeding rates, but maximum feeding rates increased more strongly with rising experimental temperature in warm adapted predators than in cold adapted predators. There was no effect of adaptation temperature on half-saturation densities characterising foraging efficiency. Besides the mixed response in functional response parameters, predators also adapted by decreasing body size. As smaller predators need less energy to fulfil their energetic demands, maximum feeding rates relative to the energetic demands increased slightly with increased adaptation temperature. Accordingly, predators adapted to 25°C showed the highest feeding rates at 25°C experimental temperature, while predators adapted to 15°C showed the highest maximum feeding rate at 15°C. Therefore, adaptation to different temperatures potentially avoids an energetic mismatch with warming. Especially a shift in body size with warming

42 additionally to an adaptation of physiological parameters potentially helps to maintain a
43 positive energy balance and prevent predator extinction with rising temperatures.

Introduction

Global change has a negative impact on biodiversity, up to a point where scientists consider the world to be on the verge of the sixth wave of mass extinction (Wake & Vredenburg, 2008; Pereira *et al.*, 2010; Barnosky *et al.*, 2011). Changing temperatures are one major driver of global change and are expected to have a global impact (MEA, 2005). Climate reports predict a minimum increase of 1.5°C in surface temperature by the end of the century and it is deemed extremely likely that anthropogenic causes (Cook *et al.*, 2013) have led to the warmest 30 year period of the last 1,400 years (IPCC, 2014). Temperature directly affects development, survival, range and abundance of species (Bale *et al.*, 2002) and has a strong effect on species interactions (Montoya & Raffaelli, 2010) as well as on the structure and dynamics of species communities (Brose *et al.*, 2012). Further, increasing temperatures in aquatic as well as terrestrial ecosystems have been linked to vast biodiversity losses during extinction waves in earlier earth periods (Gómez *et al.*, 2008; Mayhew *et al.*, 2008; Joachimski *et al.*, 2012). Despite this negative impact of high temperatures on taxonomic richness, previous periods of warming have also been associated with high speciation rates since increasing temperatures can trigger rapid evolution (Gillooly et al., 2005; Geerts et al., 2015) and create niche openings by eliminating species previously occupying a certain habitat or resource (Mayhew *et al.*, 2008). This leads to the question whether adaptation and evolution pose a feasible escape from warming induced extinction.

Species' extinctions and therewith biodiversity strongly depend on the stability of the ecosystems they are embedded in (May, 1972; McCann, 2000). Stability furthermore depends on the interaction strengths between species. High interaction strengths decreases the population stability leading to extinction caused by high population cycles, and too low an

67 interaction strength may lead to extinction of predators due to starvation (Rall *et al.*, 2010).

68 The functional response is one of the oldest and most established tools to quantify the
69 strength of these interactions and describe species-species feeding interactions in ecology
70 (Holling, 1959; Jeschke *et al.*, 2002). In this framework, the feeding rate, F, of a predator
71 depends on the density of its resource. The functional response, as described by Real
72 (1977) includes a non-linear feeding rate, which determines the maximum feeding, f, when
73 prey is abundant. At lower prey densities the functional response curve is characterised by the
74 predator's foraging efficiency. Mathematically this is described by half-saturation density, η,
75 the prey population density at which half of the maximum feeding rate is reached. (Figure 1).
76 These parameters can be used to evaluate interspecies interaction strength which have been a
77 main predictor of ecosystem stability (Berlow *et al.*, 2009).

78 To investigate the effects of warming on interaction strength, previous studies have used the
79 principles of the Metabolic Theory of Ecology (MTE) (Gillooly *et al.*, 2001; Brown *et al.*,
80 2004) which is quantified as activation energies measured in electron Volt [eV] according to
81 the Arrhenius equation (Arrhenius, 1889). The Arrhenius equation, originally used to describe
82 chemical reactions and enzyme kinetics, has become a mechanistic model for biological rates
83 in ectotherm organisms (Gillooly *et al.*, 2001; Brown *et al.*, 2004; Savage *et al.*, 2004). The
84 MTE argues that all biological rates as well as higher order patterns such as density
85 distributions scale with temperature. Therefore, the parameters of the functional response,
86 determining interaction strength should follow the same principles (Vasseur & McCann,
87 2005; Fussmann *et al.*, 2014): maximum feeding rates are often assumed to scale with
88 temperature in the same manner as metabolic demands with an activation energy ranging
89 from 0.6 to 0.7 eV across different taxa (Vasseur & McCann, 2005). This is corroborated by
90 empirical data of ciliates, flagellates and other microfauna showing even higher activation

energies for maximum feeding rates of 0.772 eV (Hansen *et al.*, 1997; Vasseur & McCann, 2005). However, a broader analysis of predators from different ecosystems revealed that maximum feeding, f, scales with an activation energy of roughly 0.3 to 0.4 eV (Rall *et al.*, 2012; Fussmann *et al.*, 2014). This leads to a mismatch where, under warming, metabolism increases faster than maximum feeding. As a result, predators cannot meet their metabolic demands and run the risk of starvation even if they are surrounded by prey (Vucic-Pestic *et al.*, 2011; Fussmann *et al.*, 2014). The half-saturation density, η, can be influenced by a variety of parameters such as encounter rate, mobility of prey and predator, and search efficiency. Most significantly, mobility of prey and predator and therefore encounter rates and search efficiencies are influenced by warming (Sentis *et al.*, 2012; Dell *et al.*, 2014). Since the reaction of prey as well as predator to changing temperatures can be highly variable in both, general tendency and intensity, this results in a high variability of activation energies for half-saturation density, ranging from positive to negative relationships with warming, being on average neutral (Fussmann *et al.*, 2014). Constant half-saturation densities can be mechanistically explained by a simultaneous increase of feeding at low densities (the "rate of successful attacks" (Holling, 1959), often referred to as attack rate, capture rate or maximum clearance rate) and maximum feeding rate with increasing temperatures. At high temperatures, natural systems show lower prey population densities due to reduced resource availability (Brown *et al.*, 2004; Meehan, 2006; Fussmann *et al.*, 2014). If predator abundances are low in natural systems and predators are not able to increase their foraging efficiency under those conditions (i.e. decrease of half-saturation densities) feeding rates eventually decrease. These mismatches can lead to the loss of higher trophic levels due to starvation (Binzer *et al.*, 2012; Fussmann *et al.*, 2014) and decreases in biodiversity due to warming (Binzer *et al.*, 2016).

115 However, other mechanisms, for example adaptation to higher temperatures, may be able to
116 counteract starvation due to energetic mismatch (Angilletta Jr., 2009; Chevin *et al.*, 2010;
117 Somero, 2010). In studies where adaptation may have buffered the physiological impacts of
118 warming, temperature had hardly any effect on the overall fitness of a population (Chown *et*
119 *al.*, 2010). Adaptation in predator-prey systems is often studied from a prey's perspective
120 (McPeek *et al.*, 1996; Yoshida *et al.*, 2003; Abrams & Walters, 2010) but rarely from a
121 predator's (Sentis *et al.*, 2015), despite them being most affected by temperature changes
122 (Rall *et al.*, 2010; Binzer *et al.*, 2012; Fussmann *et al.*, 2014). Given that predator energy
123 efficiency is a major determinant of population stability (Vasseur & McCann, 2005; Rall et
124 al., 2010), an adaptation of either metabolism or functional response parameters or both could
125 be crucial. Temperature adaptation, however, is often investigated on short time scales (Sentis
126 *et al.*, 2015) leading to concerns that the time frame of temperature changes exceeds
127 adaptation rates (Quintero & Wiens, 2013). Generally, short-term studies tend to
128 underestimate a species' capability of adapting to climate change (Leuzinger *et al.*, 2011). In a
129 short-term study focussing on acclimation within one generation, the physiological
130 temperature effect on feeding rates proved crucial since metabolic rates and body size were
131 less affected by acclimation temperature (Sentis *et al.*, 2015). However, metabolism and
132 functional response parameters are not only influenced by temperature but also by body size
133 (Vucic-Pestic *et al.*, 2011; Ott *et al.*, 2012; Rall *et al.*, 2012; Kalinkat *et al.*, 2013). However,
134 body size itself is influenced by temperature (Atkinson et al., 2003; Figure 2). Globally,
135 species in warmer regions tend to have smaller average body sizes than species in colder
136 ecosystems (Bergmann, 1847), this trend was also documented in warming studies
137 investigating different size spectra of local freshwater communities (Daufresne et al., 2009;
138 Yvon-Durocher et al., 2011). Further, body size has been shown to have a strong effect on

139 interaction strengths through allometric scaling (Brose, 2010). Smaller body sizes require less
140 energy to maintain metabolism and population growth (Brown *et al.*, 2004) leading to
141 reduced maximum feeding rates while not affecting the half-saturation densities (Hansen et
142 al., 1997). The half-saturation density ($\eta = 1/(T_h a)$) can be calculated as the inverse of the
143 product of handling time ($T_h=1/f$) and attack rate ($a = f/\eta$). Consequently, if maximum
144 feeding rates and attack rates scale similarly with body size, the effect on half-saturation
145 density is equalled out ($\eta = f/a$) (Rall *et al.*, 2012). As a result of constant half-saturation
146 density, maximum feeding rates are constant across the entire prey density gradient (Figure
147 1).

148 Here, we explored how interactive effects of direct temperature adaptation of feeding rates
149 and indirect effects on feeding rates through temperature induced changes in body size
150 influence functional response parameters. We designed a microcosm experiment with short
151 generation times (Callahan *et al.*, 2008) to understand how adaptation to different
152 temperatures over 20 generations influences feeding behaviour. We investigated whether
153 adaptation to temperature enables predator populations to avoid extinction caused by crossing
154 the threshold where metabolic demands overtake the energy intake through feeding. (1) We
155 expect body sizes of warm adapted *Tetrahymena* to decrease within 20 generations compared
156 to predators adapted to colder temperatures (Figure 2a). (2) Half-saturation densities should
157 not be affected by increasing experimental temperature. If *Tetrahymena* adapts both, attack
158 rates and maximum feeding rates simultaneously, we expect no change in half-saturation
159 density with adaptation temperature (Figure 2b). (3) The change in body size, (cell size) will
160 cause a decrease in maximum feeding rates and attack rates in warm adapted predators. Body
161 size, however, will not affect the temperature dependency of these rates or change the
162 activation energies (Figure 2c – body size mediated feeding adaptation). (4) We assume that

163 the direct physiological adaptation of maximum feeding rates and attack rates leads to a
164 change of activation energies: warm adapted predators should show the steepest increase
165 (highest activation energy) as they should be well adapted to higher temperatures. Predators
166 adapted to lower temperatures should have the highest feeding rates at cold temperatures but
167 will not or just marginally be able to increase feeding with increasing temperature (Figure 2d
168 – direct feeding adaptation). These different scalings will result in a statistically significant
169 interaction. (5) If both mechanisms occur simultaneously, maximum feeding rates and attack
170 rates should be lowest for warm adapted predators and increase with decreasing adaptation
171 temperature while keeping the interactive direct effect of adaptation (Figure 2e – realised
172 feeding adaptation).

173 Figure 1:

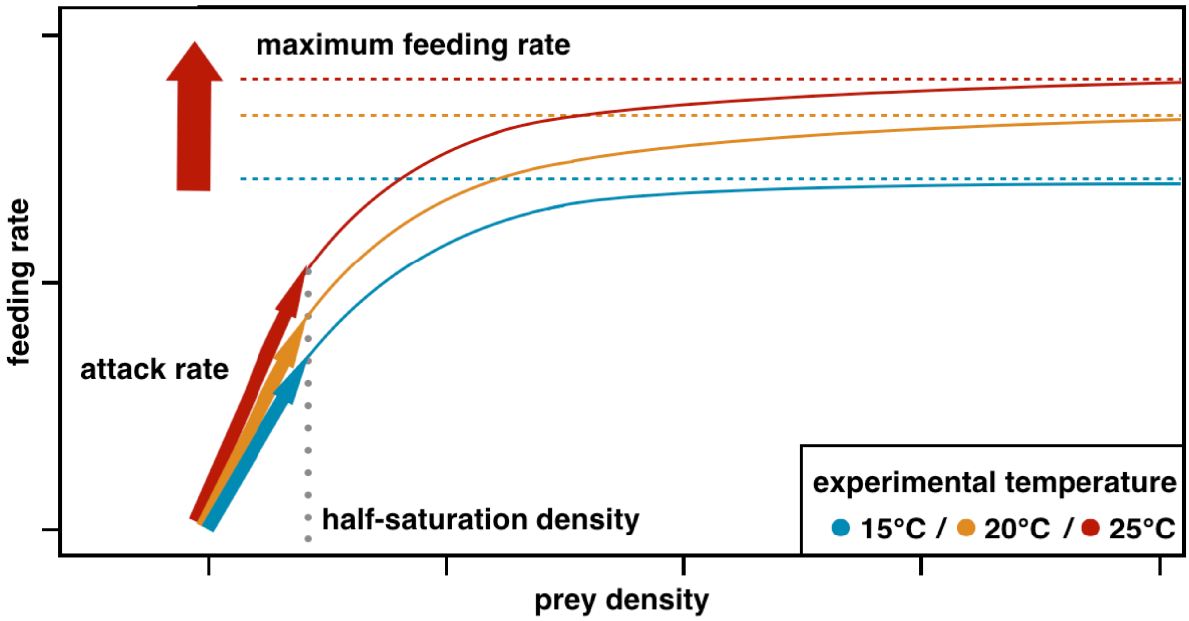

Figure 1: Expected trends for changes in maximum feeding rate (dashed lines) and half-saturation density (dotted line) with increasing temperatures based on previous studies (Rall *et al.*, 2012; Fussmann *et al.*, 2014). Maximum feeding rates are likely to increase with experimental temperature, while half-saturation densities have a variable scaling relationship being on average neutral. Maximum feeding rates of predators adapted to higher temperatures are expected to increase to cope with increasing metabolic demands with the highest maximum feeding rates at high temperatures and vice versa for cold adapted predators. Half-saturation densities are expected to not be influenced by temperature adaptation resulting in an increase of attack rates (arrows) at low prey densities in warm adapted predators to facilitate higher maximum feeding rates at high prey densities.

174 Figure 2:

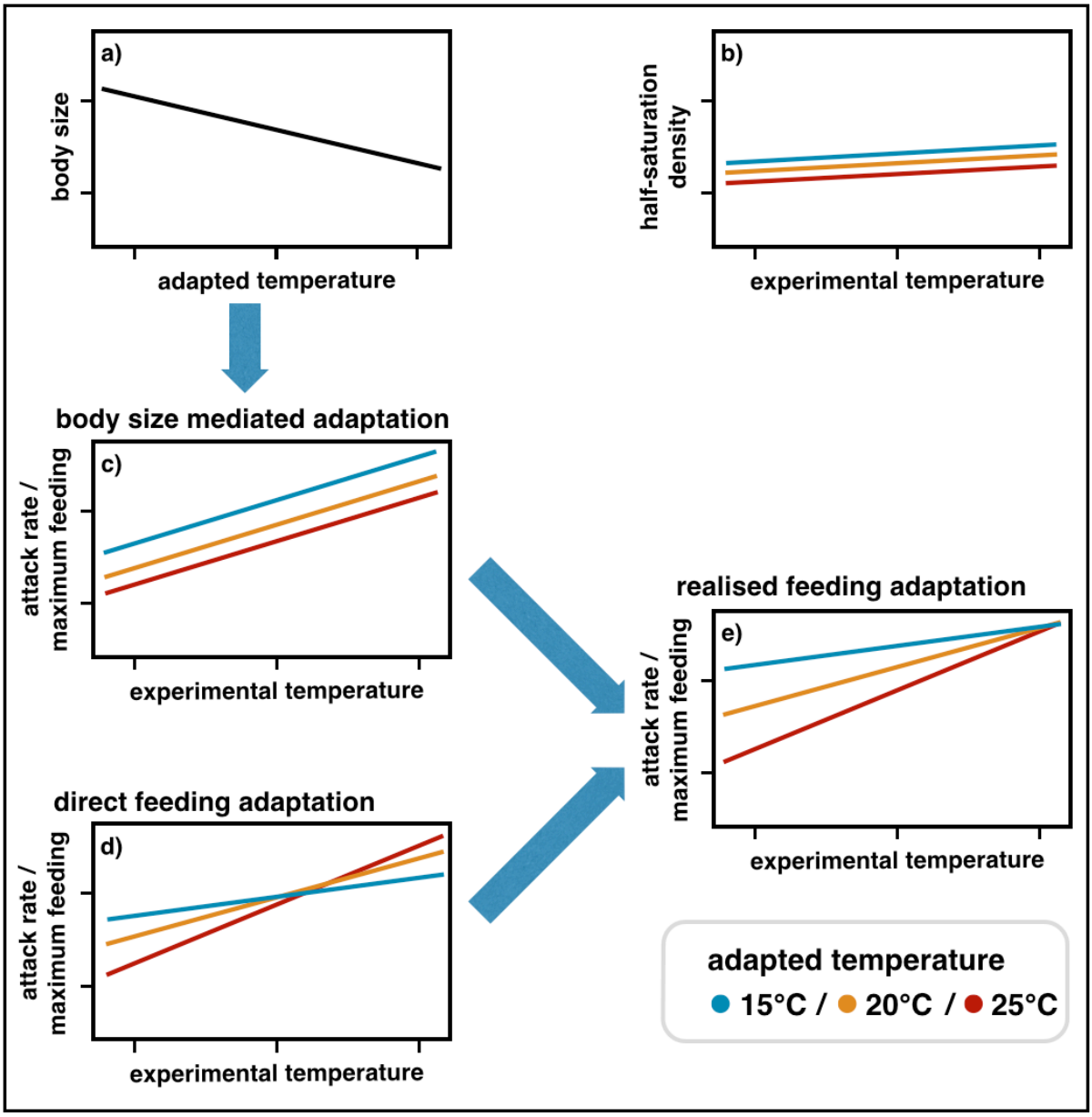

Figure 2: a) Predator body size (cell size) decreases with increasing adaptation temperature. **b) Half-saturation densities** are not expected to change with experimental or adaptation temperature. **c) Body size mediated adaptation**: Decreasing predator body size with increasing adaptation temperatures generally reduces maximum feeding rates in warm adapted predators with an assumed scaling exponent of 0.75 (Brown *et al.*, 2004). **d) Direct feeding adaptation**: Maximum feeding rates generally increase with rising experimental temperatures. Adaptation to temperature leads to a direct feeding adaptation of maximum feeding rates. Predators adapted to 15°C are expected to show the overall highest maximum feeding at 15°C experimental temperature, while predators adapted to 25°C should have the overall highest maximum feeding rates at 25°C. **e) Realised feeding adaptation:** Realised feeding adaptation shows the interactive effects of body size mediated adaptation and direct feeding adaptation on maximum feeding rates.

Methods

Laboratory Cultures:

We chose a model predator-prey system with the non-toxic bacterium *Pseudomonas fluorescens* CHA19 (Zuber *et al.*, 2003; Jousset *et al.*, 2009) as prey and the ubiquitous, predatory ciliated protozoan *Tetrahymena pyriformes* CCAP 1630/1W (CCAP Culture Collection of Algae and Protozoa, SAMS Limited, Scottish Marine Institute, Scotland, United Kingdom).

Pseudomonas fluorescens CHA19 was marked with GFP using a Mini-TN7 transposon I (Lambertsen *et al.*, 2004). After molecular cloning, one colony of the *Pseudomonas* strain was deep frozen at -80 °C in a 25 % glycerol solution. For every experiment a small sample was defrosted and incubated on LB-Agar containing 8 µg/l gentamycin before single colonies were incubated at room temperature in selective LB-medium over night. *Tetrahymena* was grown in 2% proteone peptose medium at 20°C. At the start point of the adaptation experiment, the culture of *Tetrahymena* was divided equally into 9 cultures, 3 cultures were henceforth kept at 15°C, three cultures were kept at 20°C and three cultures were kept 25°C. A temperature range between 15°C and 25°C is realistic for temperate aquatic systems in absence and presence of an extreme temperature event (Seifert *et al.*, 2015). For all adaptation temperatures, exponential growth rates of *Tetrahymena pyriformis* were measured to estimate the timeframes until approximately 20 generations were reached and functional response experiments were conducted (Supporting Information Figure 1). For predators kept at 15°C adaptation temperature, this was approximately 18 days, while for warmer adapted predators this time span was approximately 13 and 12 days for 20°C and 25°C adaptation temperature, respectively. 20 generations is consistent with other studies ranging from only

198 one generation (Sentis *et al.*, 2015) to 10 and 100 generations (Padfield *et al.*, 2015). To
199 reduce the traces of medium prior to the functional response measurements bacteria were
200 centrifuged (13.000 rpm x 1 min) and re-suspended three times in sugarless Ornston and
201 Stannier (OS) medium (Ornston, 1966) diluted with ddH2O 1:10. Bacterial counts were
202 measured using an Accuri C6 flow cytometer (BD Biosciences) on slow with an FSC-H of
203 8000 and a SSC-H of 2000. Ciliates were harvested by centrifugation at 300 rpm for 7 min at
204 0°C and re-suspended in OS medium three times. Prior to functional response experiments
205 the predators were starved for 12 hours at their respective adaptation temperatures. The
206 number of ciliates and their body sizes were measured with a Beckman Coulter Counter
207 Multisizer 4 with a 100µl aperture on slow fluidics speed (Beckman Coulter, Inc.).

208 **Functional Response Experiments**

209 Functional response experiments were conducted in 96-well plates. One column contained
210 only the ciliated predator *Tetrahymena*, each of the remaining 11 columns contained a
211 different bacterial prey density, with six rows as identical replicates and two rows as bacterial
212 controls. Each well contained 200µl of sugar-free OS 1:10 media, prey densities ranged from
213 34778 bacteria μl^{-1} to 1189416 bacteria μl^{-1}, while predator abundances were kept constant at
214 100 predators μl^{-1}. We used a fully factorial design for the functional response experiments,
215 conducting experiments at the full experimental temperature range of 15°C, 20°C and 25°C
216 with all three cultures of all adaptation temperatures after approximately 20 generations
217 (Supporting Information Figure 1). Fluorescence intensities of bacteria were measured at two
218 time points, after four hours into the experiment to avoid transient dynamics and at the end of
219 the experiment, three hours thereafter, in an Infinite M200 plate reader (Tecan, Männedorf,

Switzerland). After orbital shaking for 10 seconds, each well was measured with an excitation wavelength of 485 nm and an emission wavelength of 520 nm reading 15 flashes with a manual gain of 100. To standardise a reliable value for bacterial abundance from the GFP signal measured in the plate reader, comparative measurements were taken using a plate reader and flow cytometer with an FSC-H of 8000 and SSC-H of 2000 and slow fluidics speed.

Calculation of bacterial densities

We assessed bacterial fluorescence data by using a regression tree (tree-function, Ripley, 2016) classifying count-fluorescens relationships (Supporting Information, Figure 1).To estimate the bacterial density we first fitted the ln-transformed fluorescence signal measured in the plate reader against the ln-transformed number of cells measured with the flow cytometer (independent variable). All fluorescence values below a ln(GFP) of 6.03068 and a ln(count) of 9.071045 and above a ln(GFP) of 9.37609 and a ln(count) of 13.15602 were excluded from further analysis since we could not guarantee the proportionality between cell count and fluorescent signal beyond these counts. We then calculated bacterial abundance by predicting a linear model with GFP signal and experimental temperature as independent variables. To account for background signals, all experimental data was blanked against OS 1:10 ddH_2O experimental media and treatments containing only the predator *Tetrahymena pyriformis*. This resulted in 141 control treatments containing only bacterial prey, and 306 functional response experiments that were used for further analysis (Supporting Information Table 1).

Functional response

The functional response describing the non-linear feeding rate, F, is defined as (Real (1977):

$$F = \frac{f N}{\eta + N} \quad (1),$$

where N is the prey density, f is the maximum feeding rate and η is the half-saturation density. In our experiment, additional to a constant decline of prey through time due to feeding, natural growth and mortality of the bacterial prey occurred in control experiments. We therefore decided to incorporate a Gompertz growth for microbiological systems (Gompertz, 1825; Paine *et al.*, 2012):

$$G = rN \ln\left(\frac{K}{N}\right) \quad (2)$$

where r is the intrinsic growth rate of bacteria and K is the carrying capacity of bacteria.

A model accounting for changes in prey abundance over time due to feeding as well as natural prey growth or death is expressed in the following ordinary differential equation (ODE):

$$\frac{dN}{dt} = \frac{-f N}{\eta + N} P + rN \ln\left(\frac{K}{N}\right) \quad (3),$$

where the change in prey abundance over time t is characterised by the functional response model; P is the predator density. To account for changes of the parameters with experimental temperature we calculated Arrhenius temperatures and activation energies $E_{f,\eta}$:

$$f = f_0 e^{E_f \frac{(T_e - T_0)}{k T_e T_0}} \quad (4a),$$

$$\eta = \eta_0 e^{E_\eta \frac{(T_e - T_0)}{k T_e T_0}} \quad (4b),$$

where f_0 and η_0 are normalisation constants, T_e [K] is the absolute experimental temperature, T_0 [K] is the normalisation temperature and k [eV K^{-1}] is the Boltzmann's constant yielding the well known Arrhenius equation (Arrhenius, 1889; Gillooly *et al.*, 2001).

Additionally, growth and carrying capacity also scale with temperature (Gillooly *et al.*, 2001; Savage *et al.*, 2004):

$$r = r_0 e^{E_r \frac{(T_e - T_0)}{kT_e T_0}} \quad (4c);$$

$$K = K_0 e^{E_K \frac{(T_e - T_0)}{kT_e T_0}} \quad (4d);$$

with r_0 and K_0 being normalisation constants, and E_r and E_K being the experimental activation energies. To investigate the effects of adaptation, we extended the Arrhenius equation using a term describing the dependency of the maximum feeding rate, f, and of the half-saturation density, η, on the temperature the predator was adapted to T_a:

$$f = f_0 e^{E_f \frac{(T_e - T_0)}{kT_e T_0}} e^{A_f \frac{(T_a - T_0)}{kT_a T_0}} \quad (5a);$$

$$\eta = \eta_0 e^{E_\eta \frac{(T_e - T_0)}{kT_e T_0}} e^{A_\eta \frac{(T_a - T_0)}{kT_a T_0}} \quad (5b);$$

where A_f and A_η are the activation energies for temperature adaptation. Both, maximum feeding and half-saturation density may interactively react to both, experimental and adaptation temperature (i.e. $E_{f,\eta}$ is different for different T_a). We therefore introduced an interaction term, $I_{f,\eta}$, into equation 5a, b (i.e. statistical interaction term), yielding:

$$f = f_0 e^{E_f \frac{(T_e - T_0)}{kT_e T_0}} e^{A_f \frac{(T_a - T_0)}{kT_a T_0}} e^{I_f \frac{(T_e - T_0)}{kT_e T_0} \frac{(T_a - T_0)}{kT_a T_0}} \quad (6a);$$

$$\eta = \eta_0 e^{E_\eta \frac{(T_e - T_0)}{kT_e T_0}} e^{A_\eta \frac{(T_a - T_0)}{kT_a T_0}} e^{I_\eta \frac{(T_e - T_0)}{kT_e T_0} \frac{(T_a - T_0)}{kT_a T_0}} \quad (6b).$$

279 Further, we calculated realised activation energies for maximum feeding rates $\widetilde{E}_f$ of the
280 experimental temperature for each adaptation temperature:

281 $$\widetilde{E}_f = E_f + I_f \frac{(T_a - T_0)}{k T_a T_0} \quad (7)$$

282 Maximum feeding rates, *f*, scale not only with temperature but also with body size with a
283 power-law exponent of 0.75 according to the MTE (Yodzis & Innes, 1992; Brown *et al.*,
284 2004). Half-saturation densities, η, can be defined as the quotient of maximum feeding rate
285 and attack rate ($\eta = f/a$, Koen-Alonso, 2007), where both parameters share the same power-
286 law exponent of 0.75 (Brown *et al.*, 2004) and do not scale with body size (Yodzis & Innes,
287 1992; Hansen *et al.*, 1997).

288 The body size dependent functional response can therefore be described with a ¾ power law
289 scaling of the maximum feeding rate, *f*, with body size, *m*:

290 $$F = \frac{(f m^{0.75}) N}{\eta + N} = \left(\frac{f N}{\eta + N}\right) m^{0.75} \quad (8).$$

291 To demonstrate the effect of direct feeding adaptation (Figure 2d – direct feeding adaptation),
292 we corrected our fitted results based equation on 5a (see below and in the Supporting
293 Information a description of the fitting methods) by dividing feeding rates by the metabolic
294 body size of the predator (Schmitz & Price, 2011; Schneider *et al.*, 2012):

295 $$f_m = f_0 e^{E_f \frac{(T_e - T_0)}{k T_e T_0}} e^{A_f \frac{(T_a - T_0)}{k T_a T_0}} e^{I_f \frac{(T_e - T_0)}{k T_e T_0} \frac{(T_a - T_0)}{k T_a T_0}} / m^{0.75} \quad (9).$$

296 Mean ciliate body size [µm^3], adapted to the respective temperatures at the time of
297 experiment after an adaptation period of approximately 20 generations, was measured in the
298 Beckmann Coulter Counter. Note that this calculation was done after fitting the functional
299 response model to the data. This method to correct for body size differences in temperature

dependent functional response parameters was already successfully applied in prior studies (Sentis *et al.*, 2012, 2014).

Fitting algorithm

We used Bayesian methods for parameter estimation (equation 3 including scaling relationships for r, K, f and η). Data of prey densities after 4 hours $N(t_4)$ were used as initial values for the numerical solution of the ordinary differential equations (ODE) and data of densities after 7 hours $N(t_7)$ were modelled using ln-normally distributed errors. Model parameters for control treatments and treatments with predators present were estimated within the same model. Samples from the posterior distribution of the parameters given the data were drawn using Hamiltonian Monte Carlo sampling in Stan, accessed via the RStan package (Stan Development Team, 2016). The Stan software comes with a built in ODE-solver, making it suitable for fitting ODE-based functional responses (equation 3). We used normally distributed uninformative priors with zero means and standard deviations of 100,000 for K_0 and η_0, standard deviations of 100 for all other model parameters and a uniform distribution on the interval between 0 and 100 as a prior for the model's standard error. The parameters r_0, K_0, f_0, and η_0 were provided with a lower boundary of zero. We ran 5 Markov chains in parallel with an adaptation phase of 1,000 iterations and 20,000 sampling iterations each, summing up to 100,000 samples of the posterior distribution. Visual inspection of the trace plots and density plots showed a good mixture of the chains. Values of $\hat{R}$ sufficiently close to 1 and an adequate effective sample mass n_{eff} further verified convergence (Supporting Information, Table 3). We tested different models for including adaptation temperature in the scaling relationships of f and η (Table 1). For model comparison

we used the Watanabe-Akaike information criterion (WAIC), which can be computed from the log-likelihood values of the posterior samples by the loo package (Vehtari & Gelman, 2016). We will report results only for model 3, which performed best in the model selection (Supporting Information, Table 2). Model 3 includes an interaction term of experimental and adaptation temperature in the scaling of maximum feeding rate f, but not in the scaling of half-saturation density η. The fits of the full ODE together with the measured data points as well as functional response plots can be found in the Supporting Information (Supporting Information Figure 3 and 4). See Supporting Information also for full summary statistics, density plots and model code.

Table 1: Models for including experimental and adaptation temperature. All models include ln-linear terms of experimental temperature in the scaling of f, η, r, K (equations 4a-d).

Model	Equations	Terms for influence of adaptation temperature
1	(4a), (4b)	none
2	(5a), (5b)	ln-linear in f and η
3	(6a), (5b)	interaction with experimental temperature in f, ln-linear in η
4	(5a), (6b)	ln-linear in f, interaction with experimental temperature in η
5	(6a), (6b)	interaction with experimental temperature in f and η

Results

We found that over the course of 20 generations, predator body sizes decreased with increasing adaptation temperature, and thus predators adapted to higher temperatures had smaller average body sizes than predators kept at lower temperatures (Figure 3a). The half-saturation density (Figure 3b) generally increased with experimental temperature with no significant differences for predators adapted to different temperatures and a high variability (Table 2). According to the WAIC, model 3 (equations 6a, 5b) represented our data best, therefore, there was no interactive effect of experimental and adaptation temperature on half-saturation density. The effect of experimental temperature on half-saturation density equaled the activation energy $E_\eta = 4.359$ (with a standard deviation of 1.698 and a CI from 2.179 to 8.680) for predators adapted to all three adaptation temperatures. The effect of adaptation temperature on half-saturation density was slightly negative, but insignificant (Table 2). As half-saturation densities should not be affected by body size (Hansen et al., 1997) the direct effect of adaptation equaled the realised effect (see Figure 2). Attack rates decreased with experimental temperature, with attack rates of cold adapted predators decreasing faster than attack rates of warm adapted temperature (Supporting Information Figure 9 and Table 4, 5).

In order to calculate the direct effect of adaptation on maximum feeding rates (Figure 2d), we factored body size into the respective maximum feeding rates, a posteriori to the per capita estimation of functional response parameters (equation 8 and 9). Investigating the direct effect of adaptation on maximum feeding rates revealed that warm adapted predators had highest maximum feeding rates at the highest experimental temperatures and lowest maximum feeding rates at the lowest experimental temperature (Figure 3c). Recent studies

355 suggest a power law scaling of body size close to one for chemo-heterotrophic unicellular
356 organisms yielding the same general results (Okie et al., 2016; results shown in Supporting
357 Information, Figure 10). The physiological temperature adaptation was affecting activation
358 energies. In predators adapted to 15°C, the activation energy for maximum feeding rate
359 (equation 6a) was approximately 0.66 and increased with adaptation temperature to
360 approximately 1.05 and 1.43 for predators adapted to 20°C and 25°C, respectively (Table 3).
361 In the realised adaptation scenario, maximum feeding rates (Figure 3d) generally increased
362 with experimental temperature. Over most of the observed range of experimental
363 temperatures, maximum feeding rate was highest for predators adapted to 15°C, followed by
364 those adapted to 20°C, and lowest for those adapted to 25°C. Predators adapted to 25°C
365 showed the steepest increase in maximum feeding rate with increasing experimental
366 temperature, while predators adapted to 20°C and 15°C showed a shallower increase (Figure
367 3d). This resulted from a positive interaction between experimental and adaptation
368 temperature (Table 1). However, at 25°C experimental temperature, there was no difference
369 between maximum feeding rates of predators adapted to 15°C, 20°C or 25°C.

Table 2: Mean values of the distribution and their standard deviation for normalisation constants of maximum feeding rate f_0 and half-saturation density η_0 and their activation energy main effects of experimental temperature E_f, E_η, of adaptive temperature A_f, A_η, and the interaction term for maximum feeding rate I_f. The range between 2.5% and 97.5% of the distribution give the 95% credible intervals. For full summary statistic, please see Supporting Information Table 3.

	mean	sd	2.5%	50%	97.5%
f_0	2.654	0.085	2.505	2.647	2.841
η_0	2378.247	1932.152	83.463	1930.298	7115.469
E_f	1.054	0.056	0.950	1.052	1.168
E_η	4.359	1.698	2.179	3.976	8.680
A_f	-0.362	0.053	-0.463	-0.364	-0.252
A_η	-0.530	0.627	-1.531	-0.617	0.860
I_f	0.569	0.122	0.380	0.548	0.855

Table 3: Median of estimated activation energies of maximum feeding rate (equation 7) for the ciliate predator *Tetrahymena pyriformis* adapted to 15°C, 20°C and 25°C for approximately 20 generations.

adaptation temperature	*activation energy*
	maximum feeding rate
15°C	0.663
20°C	1.054
25°C	1.431

379 **Figure 3:**

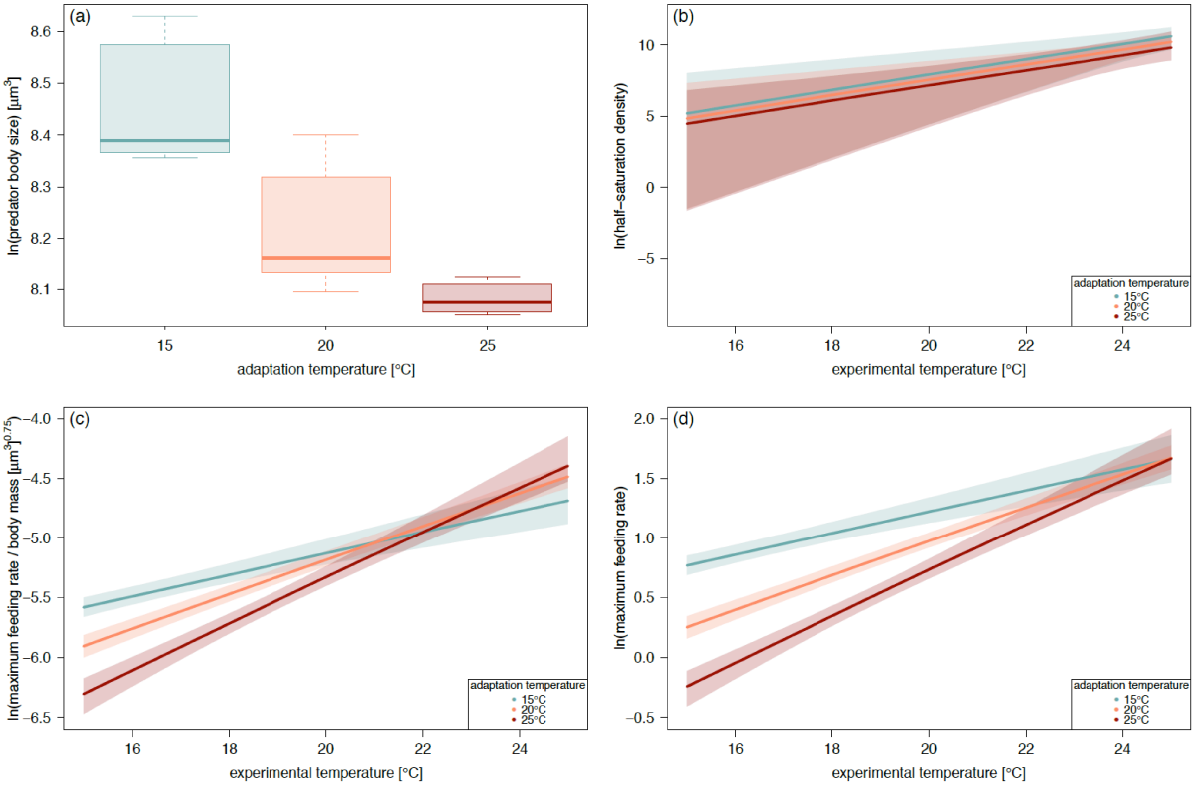

Figure 3: a) Body sizes of *Tetrahymena pyriformis* adapted to 15°C, 20°C and 25°C in µm³ measured in the Beckmann Coulter Counter decreased with adaptation temperature. **b) Half-saturation densities** for *Tetrahymena pyriformis* adapted to 15°C (blue), 20°C (orange) and 25°C (red) increased with experimental temperature. There was no significant difference for half-saturation density between predators adapted to different temperatures along the gradient of experimental temperatures. **c) Metabolic body-size accounted maximum feeding rates** (f / body size$^{0.75}$ [µm³]) for *Tetrahymena pyriformis* adapted to 15°C , 20°C and 25°C along an experimental temperature gradient showed an increase with experimental temperature while predators adapted to 15°C and 25°C showed the highest maximum feeding rates at their adaptation temperature, respectively. **d) Maximum feeding rates** for *Tetrahymena pyriformis* adapted to 15°C , 20°C and 25°C increased with experimental temperatures. While maximum feeding rates slightly decreased with adaptation temperatures, predators adapted to 25°C over 20 generations showed the strongest increase in maximum feeding with experimental temperature due to a positive interaction effect of experimental and adaptation temperature. Solid lines represent median values, shaded areas indicate 95% credibility intervals.

Discussion

Increasing temperatures are putting a strain on biodiversity in ecosystems world wide. Previous studies have revealed an increasing mismatch between maximum feeding rates and metabolism with warming as an often overlooked and until recently poorly understood cause of extinction (Vucic-Pestic *et al.*, 2011; Rall *et al.*, 2012; Fussmann *et al.*, 2014).

Here, we investigated the effect of possible temperature adaptations on feeding interactions. After an adaptation period of approximately 20 generations, predator body size had decreased significantly for predators adapted to 25°C compared to predators kept at the lowest adaptation temperature according to our prediction based on previous studies (Bergmann, 1847; Daufresne *et al.*, 2009; Yvon-Durocher *et al.*, 2011). We ran functional response experiments along a temperature gradient with predators adapted to different temperature regimes and found that experimental temperature has an effect on half-saturation densities of predators adapted to all three adaptation temperatures (Fussmann *et al.*, 2014). Using more than one predator per experimental treatment, the particularly high values of half-saturation densities might be explained by predator interference. Interference has been observed among unicellular organisms (Curds & Cockburn, 1968) and can be affected by temperature changes (Lang *et al.*, 2012). By reducing the time available for prey encounters, interference lowers the feeding efficiency of predators (Abrams & Ginzburg, 2000). In cases where half-saturation density and interference both increase with warming, this could lead to a combined effect on half-saturation densities. Declining attack rates with experimental temperature can be caused by increasing interference and therefore corroborate this assumption. However, since we did not vary predator density to manipulate the strength of predator interference, this can only be speculated. According to our model comparison there is no interactive effect of

403 experimental and adaptation temperature on half-saturation density. This suggests, that the
404 effect of adaptation temperature on half-saturation-density is buffered by a simultaneous
405 temperature adaptation of attack rate and maximum feeding rate. Therefore, adaptation of
406 half-saturation densities should be excluded as a possible mechanism to counteract
407 temperature effects on carrying capacities and decreasing prey abundances at higher
408 temperatures in natural systems. However, predators adapted to higher temperatures show the
409 steepest increase of maximum feeding rate with increasing experimental temperature
410 enabling them to react to increasing temperatures quicker and increase their energy intake
411 faster within the measured temperature range. Predators adapted to 25°C show lower
412 maximum feeding rates at 15°C and 20°C than cold adapted predators, while at 25°C
413 experimental temperature, all predators show similar maximum feeding rates. In our
414 experiment we were unable to document potential changes in metabolism for predators
415 adapted to different adaptation temperatures, which leaves two possible hypotheses to explain
416 our findings. The hypothesis that metabolic rates were unaffected by adaptation temperature
417 leads to the conclusion that predators adapted to higher temperatures have gained a
418 disadvantage at lower experimental temperatures becoming less efficient compared to their
419 cold adapted counterparts, while there is no clear advantage gained at high experimental
420 temperatures. However, due to smaller body sizes of warm adapted predators, predators
421 adapted to 25°C adaptation temperature are expected to have lower metabolic demands
422 compared to cold adapted predators, if any potential physiological adaptation of metabolism
423 is taken into account (Brown *et al.*, 2004). Relevantly, our experimental units contained more
424 than one predator individual, these lowered metabolic demands can lead to an increase in
425 predator interference, reducing maximum feeding rates at low experimental temperatures.
426 With increasing experimental temperatures, these predators will prioritise feeding over

427 predator interaction leading to the strong increase of maximum feeding rates with
428 experimental temperature in warm adapted predators. While some studies predict activation
429 energies for maximum feeding rates ranging from 0.6-0.7 eV, our results are in the range of
430 activation energies reported for ciliated protozoan and other unicellular organisms around
431 0.772 eV (Hansen *et al.*, 1997; Vasseur & McCann, 2005). Activation energies for
432 metabolism drawn from respiration measurements by Laybourn & Finlay (1976) of 0.96 eV
433 (Fussmann *et al.*, 2014), match the range of activation energies of maximum feeding rates in
434 our functional response measurement. Predators adapted to 20°C and 25°C show higher
435 activation energies to counteract increasing metabolic demands at higher temperatures.
436 Combining the strong increase in maximum feeding rate with the change in intercept caused
437 by body size adaptation, these results are in line with the hypothesised interactive effect of
438 body size adaptation, and adaptation temperature and experimental warming on maximum
439 feeding rates.

440 Over the timespan of 20 generations, our results as well as previous studies have shown that
441 adaptation to increased temperatures influences protist body sizes (Atkinson *et al.*, 2003)
442 highlighting the importance of trans-generational studies regarding not only genetic
443 adaptation but also phenotypic changes (DeLong *et al.*, 2016). Larger species, predominantly
444 found at higher trophic levels (Riede *et al.*, 2011) are most vulnerable to extinction due to an
445 energetic mismatch with increasing temperatures (Binzer *et al.*, 2012). This leads to a shift
446 towards smaller species in aquatic systems (Daufresne *et al.*, 2009; Yvon-Durocher *et al.*,
447 2011). The relationship between increasing predator body size and maximum feeding rate
448 follows a ¾ power-law scaling (Hansen *et al.*, 1997; Rall *et al.*, 2012), leading to lower
449 maximum feeding rates in smaller predators. To disentangle the indirect effect of predator
450 body size on the realised maximum feeding rate from the direct effect of physiological

451 adaptation we corrected our results accordingly (see figure 2 and equations 8 and 9 for a
452 detailed derivation). Once this change in body size is accounted for, we found that at 25°C
453 experimental temperature, maximum feeding rates shift towards a scenario that suggest a
454 specialised temperature adaptation of predators. While at 15°C predators adapted to that
455 temperature show the highest maximum feeding rates, at 25°C predators adapted to 25°C
456 show the highest maximum feeding rates. There is not one culture adapted to have the best
457 fitness at the full temperature range, rather predators seemed to be adapted to their respective
458 temperature. The direct physiological adaptation of maximum feeding rates leads to a
459 stronger increase in maximum feeding rate with experimental temperature in warm adapted
460 predators. Further, in form of a morphological adaptation to warming, with a smaller average
461 body size, predators increase per-biomass consumption while reducing metabolic demand.
462 This increases the effect of physiological adaptation of maximum feeding rates, resulting in a
463 combined effect increasing overall energy efficiency in warm adapted predators at high
464 temperatures.

465 In conclusion, our results suggest that while un-adapted predators face a mismatch between
466 maximum feeding rates and metabolic demands with increasing temperatures leading to
467 starvation and extinction of predators, adaptation poses a viable escape from this scenario. By
468 decreasing their body size over the course of 20 generations at higher temperatures, predators
469 lower their per-capita metabolic rates. Therefore, the ratio between metabolic costs and
470 maximum feeding rates increases for warm adapted predators, decreasing their risk of
471 starvation. The decrease in the risk of starvation also implies a decreased risk of extinction
472 which may buffer expected biodiversity loss with climate warming and increased ecosystem
473 stability.

474 It is widely accepted that adaptation occurs within ecological time spans and is therefore of

475 utmost importance for the understanding of population stability and ecosystem dynamics
476 under the threat of an increasingly fast changing environment (Holt, 1990; Lynch & Lande,
477 1993; Burger & Lynch, 1995; Merilä, 2012; Merilä & Hendry, 2014). Especially in a
478 homogeneous environment like water, where stressors cannot be avoided by migration or
479 refuge in microhabitats, the strain of climate change poses a particularly high risk for
480 populations (Bergmann *et al.*, 2010). Adaptation might be a possible way for populations to
481 deal with increasing temperatures and persist in a warming environment.

482 Acknowledgements:

483 K.E.F. received funding from the Dorothea Schlözer Programme of Göttingen University.
484 K.E.F., B.R., U.B. and B.C.R. gratefully acknowledge the support of the German Centre for
485 Integrative Biodiversity Research (iDiv) Halle-Jena-Leipzig funded by the German Research
486 Foundation (FZT 118). We would like to thank A.Binzer and D.Perkins for helpful
487 suggestions and comments.

References:

Abrams PA, Ginzburg LR (2000) The nature of predation: prey dependent, ratio dependent or neither? *Trends in Ecology and Evolution*, **15**, 337–341.

Abrams PA, Walters CJ (2010) Invulnerable prey and the paradox of enrichment. *Ecology*, **77**, 1125–1133.

Angilletta Jr. MJ (2009) Looking for answers to questions about heat stress: researchers are getting warmer. *Functional Ecology*, **23**, 231–232.

Arrhenius S (1889) Über die Reaktionsgeschwindigkeit bei der Inversion von Rohrzucker durch Säuren. *Zeitschrift für Physikalische Chemie*, **4**, 226–248.

Atkinson D, Ciotti BJ, Montagnes DJS (2003) Protists decrease in size linearly with temperature: ca. 2.5% $°C^{-1}$. *Proceedings of the Royal Society B: Biological Sciences*, **270**, 2605–2611.

Bale JS, Masters GJ, Hodkinson ID et al. (2002) Herbivory in global climate change research: direct effects of rising temperature on insect herbivores. *Global Change Biology*, **8**, 1–16.

Barnosky AD, Matzke N, Tomiya S et al. (2011) Has the earth's sixth mass extinction already arrived? *Nature*, **471**, 51–57.

Bergmann C (1847) Über die Verhältnisse der Wärmeökonomie der Thiere zu ihrer Grösse. 595–708 pp.

Bergmann N, Winters G, Rauch G et al. (2010) Population-specificity of heat stress gene induction in northern and southern eelgrass *Zostera marina* populations under simulated global warming. *Molecular Ecology*, **19**, 2870–83.

Berlow EL, Dunne JA, Martinez ND, Stark PB, Williams RJ, Brose U (2009) Simple prediction of interaction strengths in complex food webs. *Proceedings of the National Academy of Sciences of the United States of America*, **106**, 187–191.

Binzer A, Guill C, Brose U, Rall BC (2012) The dynamics of food chains under climate change and nutrient enrichment. *Philosophical Transactions of the Royal Society B: Biological Sciences*, **367**, 2935–2944.

Binzer A, Guill C, Rall BC, Brose U (2016) Interactive effects of warming, eutrophication and size structure: impacts on biodiversity and food-web structure. *Global Change Biology*, **22**, 220–227.

Brose U (2010) Body-mass constraints on foraging behaviour determine population and food-web dynamics. *Functional Ecology*, **24**, 28–34.

Brose U, Dunne JA, Montoya JM, Petchey OL, Schneider FD, Jacob U (2012) Climate

change in size-structured ecosystems. *Philosophical Transactions of the Royal Society B: Biological Sciences*, **367**, 2903–2912.

Brown JH, Gillooly JF, Allen AP, Savage VM, West GB (2004) Toward a metabolic theory of ecology. *Ecology*, **85**, 1771–1789.

Burger R, Lynch M (1995) Evolution and extinction in a changing environment: a quantitative-genetic analysis. *Evolution*, **49**, 151–163.

Callahan HS, Maughan H, Steiner UK (2008) Phenotypic plasticity, costs of phenotypes, and costs of plasticity: toward an integrative view. *Annals of the New York Academy of Sciences*, **1133**, 44–66.

Chevin L-M, Lande R, Mace GM (2010) Adaptation, plasticity, and extinction in a changing environment: towards a predictive theory. *PLoS Biology*, **8**, e1000357.

Chown SL, Hoffmann A a., Kristensen TN, Angilletta MJ, Stenseth NC, Pertoldi C (2010) Adapting to climate change: a perspective from evolutionary physiology. *Climate Research*, **43**, 3–15.

Cook J, Nuccitelli D, Green SA et al. (2013) Quantifying the consensus on anthropogenic global warming in the scientific literature. *Environmental Research Letters*, **8**, 24024.

Curds CR, Cockburn A (1968) Studies on the growth and feeding of *Tetrahymena pyriformis* in axenic and monoxenic culture. *Journal of General Microbiology*, **54**, 343–358.

Daufresne M, Lengfellner K, Sommer U (2009) Global warming benefits the small in aquatic ecosystems. *Proceedings of the National Academy of Sciences of the United States of America*, **106**, 12788–12793.

Dell AI, Pawar S, Savage VM (2014) Temperature dependence of trophic interactions are driven by asymmetry of species responses and foraging strategy. *Journal of Animal Ecology*, **83**, 70–84.

DeLong JP, Forbes VE, Galic N, Gibert JP, Laport RG, Phillips JS, Vavra JM (2016) How fast is fast? Eco-evolutionary dynamics and rates of change in populations and phenotypes. *Ecology and Evolution*, **68588**, 1–9.

Fussmann KE, Schwarzmüller F, Brose U, Jousset A, Rall BC (2014) Ecological stability in response to warming. *Nature Climate Change*, **4**, 206–210.

Geerts AN, Vanoverbeke J, Vanschoenwinkel B et al. (2015) Rapid evolution of thermal tolerance in the water flea *Daphnia*. *Nature Climate Change*, **5**, 665–668.

Gillooly JF, Brown JH, West GB, Savage VM, Charnov EL (2001) Effects of size and temperature on metabolic rate. *Science*, **293**, 2248–2251.

Gómez JJ, Goy A, Canales ML (2008) Seawater temperature and carbon isotope variations in

556 belemnites linked to mass extinction during the Toarcian (Early Jurassic) in central and
557 northern Spain *Palaeogeography, Palaeoclimatology, Palaeoecology*, **258**, 28–58.

558 Gompertz B (1825) On the nature of the function expressive of the law of human mortality,
559 and on a new mode of determining the value of life contingencies. *Philosophical*
560 *Transactions of The Royal Society of London*, **115**, 513–583.

561 Hansen PJ, Bjørnsen PK, Hansen BW (1997) Zooplankton grazing and growth: scaling
562 within the 2-2,000 µm body size range. *Limnology and Oceanography*, **42**, 687–704.

563 Holling CS (1959) Some characteristics of simple types of predation and parasitism. *The*
564 *Canadian Entomologist*, **91**, 385–398.

565 Holt RD (1990) The microevolutionary consequences of climate change. *Trends in Ecology*
566 *& Evolution*, **5**, 311–315.

567 IPCC (2014) *Climate Change 2014: Synthesis Report. Contribution of Working Groups I, II*
568 *and III to the Fifth Assessment Report of the Intergovernmental Panel on Climate*
569 *Change*. 151 pp.

570 Jeschke JM, Kopp M, Tollrian R (2002) Predator functional responses: discriminating
571 between handling and digesting prey. *Ecological Monographs*, **72**, 95–112.

572 Joachimski MM, Lai X, Shen S et al. (2012) Climate warming in the latest Permian and the
573 Permian-Triassic mass extinction. *Geology*, **40**, 195–198.

574 Jousset A, Rochat L, Péchy-Tarr M, Keel C, Scheu S, Bonkowski M (2009) Predators
575 promote defence of rhizosphere bacterial populations by selective feeding on non-toxic
576 cheaters. *The ISME Journal*, **3**, 666–674.

577 Kalinkat G, Schneider FD, Digel C, Guill C, Rall BC, Brose U (2013) Body masses,
578 functional responses and predator-prey stability. *Ecology Letters*, **16**, 1126–1134.

579 Koen-Alonso M (2007) A process-oriented approach to the multispecies functional response.
580 *From Energetics to Ecosystems: The Dynamics and Structure of Ecological Systems*, 1–
581 36.

582 Lambertsen L, Sternberg C, Molin S (2004) Mini-Tn7 transposons for site-specific tagging of
583 bacteria with fluorescent proteins. *Environmental Microbiology*, **6**, 726–732.

584 Lang B, Rall BC, Brose U (2012) Warming effects on consumption and intraspecific
585 interference competition depend on predator metabolism. *Journal of Animal Ecology*,
586 **81**, 516–523.

587 Laybourn J, Finlay BJ (1976) Respiratory energy losses related to cell weight and
588 temperature in ciliated protozoa. *Oecologia*, **24**, 349–355.

589 Leuzinger S, Luo Y, Beier C, Dieleman W, Vicca S, Körner C (2011) Do global change

experiments overestimate impacts on terrestrial ecosystems? *Trends in Ecology and Evolution*, **26**, 236–241.

Lynch M, Lande R (1993) Evolution and extinction in response to environmental change *Biotic Interactions and Global Change*, pp. 234–250.

May RM (1972) Will a large complex system be stable? *Nature*, **238**, 413–414.

Mayhew PJ, Jenkins GB, Benton TG (2008) A long-term association between global temperature and biodiversity, origination and extinction in the fossil record. *Proceedings of The Royal Society*, **275**, 47–53.

McCann KS (2000) The diversity-stability debate. *Nature*, **405**, 228–233.

McPeek MA, Schrot AK, Brown JM (1996) Adaptation to predators in a new community: swimming performance and predator avoidance in damselflies. *Ecology*, **77**, 617–629.

MEA (2005) Ecosystems and human well-being health synthesis. *Ecosystems*, **5**, 1–100.

Meehan TD (2006) Energy use and animal abundance in litter and soil communities. *Ecology*, **87**, 1650–1658.

Merilä J (2012) Evolution in response to climate change: in pursuit of the missing evidence. *BioEssays*, **34**, 811–818.

Merilä J, Hendry AP (2014) Climate change, adaptation, and phenotypic plasticity: the problem and the evidence. *Evolutionary Applications*, **7**, 1–14.

Montoya JM, Raffaelli D (2010) Climate change, biotic interactions and ecosystem services. *Philosophical Transactions of the Royal Society B-Biological Sciences*, **365**, 2013–2018.

Okie JG, Smith VH, Martin-Cereceda M (2016) Major evolutionary transitions of life, metabolic scaling and the number and size of mitochondria and chloroplasts. *Proceedings of The Royal Society B*, **283**.

Ornston LN (1966) The conversion of catechol and protocatechuate to beta-oxadipate by *Pseudomonas putida*. IV. Regulation. *Journal of Biological Chemistry*, **241**, 3800–3810.

Ott D, Rall BC, Brose U (2012) Climate change effects on macrofaunal litter decomposition: the interplay of temperature, body masses and stoichiometry. *Philosophical Transactions of the Royal Society B: Biological Sciences*, **367**, 3025–3032.

Padfield D, Yvon-Durocher G, Buckling A, Jennings S, Yvon-Durocher G (2015) Rapid evolution of metabolic traits explains thermal adaptation in phytoplankton. *Ecology Letters*, 1–10.

Paine CET, Marthews TR, Vogt DR, Purves D, Rees M, Hector A, Turnbull LA (2012) How to fit nonlinear plant growth models and calculate growth rates: an update for ecologists. *Methods in Ecology and Evolution*, **3**, 245–256.

624 Pereira HM, Leadley PW, Proença V et al. (2010) Scenarios for global biodiversity in the 21st
625 century. *Science*, **330**, 1496–1501.

626 Quintero I, Wiens JJ (2013) Rates of projected climate change dramatically exceed past rates
627 of climatic niche evolution among vertebrate species. *Ecology Letters*, **16**, 1095–1103.

628 Rall BC, Vucic-Pestic O, Ehnes RB, Emmerson M, Brose U (2010) Temperature, predator-
629 prey interaction strength and population stability. *Global Change Biology*, **16**, 2145–
630 2157.

631 Rall BC, Brose U, Hartvig M, Kalinkat G, Schwarzmüller F, Vucic-Pestic O, Petchey OL
632 (2012) Universal temperature and body-mass scaling of feeding rates. *Philosophical*
633 *Transactions of the Royal Society B: Biological Sciences*, **367**, 2923–2934.

634 Real LA (1977) The Kinetics of Functional Response. *The American Naturalist*, **111**, 289–
635 300.

636 Riede JO, Binzer A, Brose U, de Castro F, Curtsdotter A, Rall BC, Eklöf A (2011) Size-based
637 food web characteristics govern the response to species extinctions. *Basic and Applied*
638 *Ecology*, **12**, 581–589.

639 Ripley B (2016) tree: Classification and Regression Trees.

640 Savage VM, Gilloly JF, Brown JH, Charnov EL (2004) Effects of body size and temperature
641 on population growth. *The American Naturalist*, **163**, 429–441.

642 Schmitz OJ, Price JR (2011) Convergence of trophic interaction strengths in grassland food
643 webs through metabolic scaling of herbivore biomass. *Journal of Animal Ecology*, **80**,
644 1330–1336.

645 Schneider FD, Scheu S, Brose U (2012) Body mass constraints on feeding rates determine the
646 consequences of predator loss. *Ecology Letters*, **15**, 436–443.

647 Seifert LI, Weithoff G, Gaedke U, Vos M (2015) Warming-induced changes in predation,
648 extinction and invasion in an ectotherm food web. *Oecologia*.

649 Sentis A, Hemptinne J-L, Brodeur J (2012) Using functional response modelling to
650 investigate the effect of temperature on predator feeding rate and energetic efficiency.
651 *Oecologia*, **169**, 1117–1125.

652 Sentis A, Hemptinne JL, Brodeur J (2014) Towards a mechanistic understanding of
653 temperature and enrichment effects on species interaction strength, omnivory and food-
654 web structure. *Ecology Letters*, **17**, 785–793.

655 Sentis A, Morisson J, Boukal DS (2015) Thermal acclimation modulates the impacts of
656 temperature and enrichment on trophic interaction strengths and population dynamics.
657 *Global Change Biology*, **21**, 3290–3298.

658 Somero GN (2010) The physiology of climate change: how potentials for acclimatization and
659 genetic adaptation will determine "winners" and "losers". *The Journal Of Experimental*
660 *Biology*, **213**, 912–920.

661 Stan Development Team RStan: the R interface to Stan. Version 2.9.0. (2016).

662 Vasseur DA, McCann KS (2005) A mechanistic approach for modelling temperature-
663 dependent consumer-resource dynamics. *The American Naturalist*, **166**, 184–198.

664 Vehtari A, Gelman A (2016) Practical Bayesian model evaluation using leave-one-out cross-
665 validation and estimating out-of-sample pointwise predictive accuracy using posterior
666 simulations.

667 Vucic-Pestic O, Ehnes RB, Rall BC, Brose U (2011) Warming up the system: higher predator
668 feeding rates but lower energetic efficiencies. *Global Change Biology*, **17**, 1301–1310.

669 Wake DB, Vredenburg VT (2008) Colloquium paper: are we in the midst of the sixth mass
670 extinction? A view from the world of amphibians. *PNAS*, **105**, 11466–11473.

671 Yodzis P, Innes S (1992) Body size and consumer-resource dynamics. *The American*
672 *Naturalist*, **139**, 1151–1175.

673 Yoshida T, Jones LE, Ellner SP, Fussmann GF, Hairston NG (2003) Rapid evolution drives
674 ecological dynamics in a predator-prey system. *Nature*, **424**, 303–306.

675 Yvon-Durocher G, Reiss J, Blanchard J et al. (2011) Across ecosystem comparisons of size
676 structure: methods, approaches and prospects. *Oikos*, **120**, 550–563.

677 Zuber S, Carruthers F, Keel C et al. (2003) GacS sensor domains pertinent to the regulation of
678 exoproduct formation and to the biocontrol potential of *Pseudomonas fluorescens*
679 CHA0. *Molecular Plant-Microbe Interactions,* **16**, 634–644.